



Variation of micellization, thermodynamic, and surface properties of sodium dodecyl sulfate in aqueous media using 1,3-disulfo-2-alkyl imidazolium chloride ionic liquids

Debanga Bhusan Bora¹ · Bhaskar Ranjan Bora¹ · Subham Paul¹ · Sangeeta Kalita¹ · Niharika Kashyap¹ · Ruli Borah¹

Received: 5 December 2023 / Revised: 8 February 2024 / Accepted: 4 March 2024 / Published online: 23 March 2024
© The Author(s), under exclusive licence to Springer-Verlag GmbH Germany, part of Springer Nature 2024

Abstract

Three direct $-NSO_3H$ functionalized Brønsted acidic ionic liquids of 2-alkyl-1,3-disulfo imidazolium chloride with varied sizes of alkyl substituents (Me-, Et-, nBu-) were utilized to explore the effects of ionic liquids on aggregation behavior of anionic surfactant sodium dodecyl sulfate in aqueous media at various concentrations of ionic liquids and temperatures (288.15 K, 293.15 K, 298.15 K, 303.15 K, and 308.15 K). Critical micelle concentrations (CMCs) of the IL-surfactant systems obtained from conductivity measurement were found to be in good agreement with the CMC values of surface tension and UV-visible spectroscopy techniques. These CMCs values were used to calculate the thermodynamic parameters of IL-surfactant solutions such as standard free energy of micellization (ΔG_m°), standard enthalpy of micellization (ΔH_m°), and standard entropy of micellization (ΔS_m°). Continuous decrease of the CMC values was observed with increasing concentrations of the ILs as well as temperatures. Packing parameters calculated from the surface tension measurement displayed small spherical shape for all the mixed micellar systems. Structural changes of the IL-surfactant solutions were also observed using FT-IR spectroscopic method. Increased positive inductive effect (+I) of 2-alkyl substituent of the imidazolium cation of ionic liquid showed stabilizing effect on the micelle formation by lowering of more negative zeta potential values of the IL-surfactant systems.

Keywords Anionic surfactant · Micellization · Critical micelle concentration · Acidic ionic liquids · Thermodynamic parameters · Surface properties

Abbreviations

SDS	Sodium dodecyl sulfate
CMC	Critical micelle concentration
ILs	Ionic liquids
BAILs	Brønsted acidic ionic liquids (BAILs)
BDSIM	2-Butyl-1,3-disulfoimidazolium (BDSIM)
EDSIM	2-Ethyl-1,3-disulfoimidazolium
MDSIM	2-Methyl-1,3-disulfoimidazolium

Introduction

Self-assembling of amphiphilic molecules [1] like surfactant in solution has received substantial research attention because of their widespread applications including

cosmetics [2], detergents [3], pharmaceuticals [4], food industry [5], nanotechnology [6–8], petroleum industry [9], and in biochemical analysis [10, 11]. Surfactants possess hydrophilic head groups and long hydrophobic tail components and can reduce interfacial tension between two dissimilar phases including liquid–liquid, gas–liquid, gas–solid, or liquid–solid interfaces through self-aggregation with formation of varied structures of micelles, vesicles, etc., above the critical micellar concentration (CMC) at fixed temperature and pressure [1, 12]. The physicochemical properties of surfactant molecules to self-assemble in aqueous medium can be tuned using various additives such as ionic liquids, inorganic salts, change of temperature, nature of counter-ions, etc. [13–15]. The change of micellization behavior of these surfactant solutions depends on the nature of head group, hydrophobic chain length, and types of interactions that prevail in the system in addition to pH of the solution [16–18].

In this context, several studies have been carried out by mixing of aqueous surfactant solution with ionic liquid to get unusual physicochemical properties of micellization along with varied structures of aggregates [19–21] based

✉ Ruli Borah
ruli@tezu.ernet.in

¹ Department of Chemical Sciences, Tezpur University, Napaam-784028 Tezpur, Assam, India

on their composition ratios that are different from individual components [22–24]. The literature of ionic liquids reveals that they represent a prospective class of materials with wide range of uses as catalysts, solvents, electrolytes, extractants, plasticizers, lubricants, and many more [25–29]. Ionic liquids are organic salts composed of organic cations in association with organic or inorganic anions and exist in liquid state below 100 °C. They show unique and variable physicochemical properties achievable by proper selection of the constituent ion-pair of IL to get the desired properties. These properties incorporate non-flammability, non-volatility, viscosity, wide thermal stability range, power to dissolve organic/inorganic substrates, variation of task specific nature such as acidities, hydrophilic/hydrophobic behavior, water stability, self-aggregation, solvatochromic parameters, ionic conductivity, electrochemical stability windows, etc. [26–30]. For example, long alkyl chain tethered ILs behave as distinctive surfactants in water by reducing surface tension of solvent and thus self-assemble to micelles when dissolved in water [31, 32]. Similarly, the attachment of structural functionalities like $-\text{SO}_3\text{H}$ or $-\text{COOH}$ groups either to the cation, anion, or both the ions of ILs makes them Brønsted acidic nature and thus behaves not only as reaction medium but serves secondary functions such as a catalyst or as reactant [33, 34]. Therefore, the addition of ILs to surfactant solutions provides them the capability to regulate surface and thermodynamic parameters of the aqueous surfactant solution involving electrostatic and hydrophobic interactions between them [35–37].

By following this, many bodies of literature have been observed to investigate the aggregation behavior of mixtures of the ILs and surfactants in solution (cationic, anionic, and non-ionic) [38–40]. In 2004, Beyaz and his co-workers investigated the variation of aggregation behavior of SDS in aqueous solutions in presence of 1,3-dialkyl imidazolium halide with varied hydrophobicity using UV–Vis spectroscopic method [41]. In two different studies, Behera et al. observed the effects of hydrophilic 1-butyl-3-methylimidazolium tetrafluoroborate [bmim][BF₄] and hydrophobic 1-butyl-3-methylimidazolium hexafluorophosphate [bmim][PF₆] ionic liquids on micellization of the aqueous SDS by conductivity and fluorescence methods [42, 43]. The decreasing trend of CMCs at lower concentrations, i.e., ≤ 2 wt% of [bmim][BF₄] and ≤ 0.1 wt% of [bmim][PF₆], reflected their action as common electrolytes in contrast to their behavior as polar co-solvents above these concentrations through involvement in growth of the SDS micelles. Another study also reported the reduction of CMCs of aqueous SDS mixtures containing 1-alkyl-3-methyl imidazolium salts [C_nmim]X, where $n = 4, 6, 10$ and $X = \text{PF}_6^-, \text{BF}_4^-, \text{and Br}^-$ with rising concentration of the ILs in the mixtures for change of electrostatic and hydrophobic interactions [44]. The solvophobic

interactions between SDS and 3-methyl-5-methylimidazolium hexafluorophosphate [C₅mim][PF₆] can also be expected for increase in the CMCs of SDS due to formation of mixed micelles [45]. Ferreira et al. in 2015 studied the micellization behavior of aqueous SDS in presence of 1-butyl-3-methylimidazolium halide SDS by conductivity, fluorescence, and calorimetry methods and displayed the decrease of CMC values of SDS with the rise of IL concentrations [46]. Kumar et al. [47] in 2021 determined the CMCs of SDS in aqueous 1-butyl-3-methylimidazolium chloride [C₄mim][Cl] solution at 298.15 K and estimated various thermodynamical parameters of micellization like standard enthalpy of micellization, standard free energy of micellization, and standard entropy of micellization. It was observed that with increasing concentration of the IL and temperature, the CMCs of SDS solution increase. The same type of study was also extended to observe the effect of imidazolium ILs for change of aggregation behavior as well thermodynamic properties of anionic surfactant sodium hexadecyl sulfate (SHS) [48].

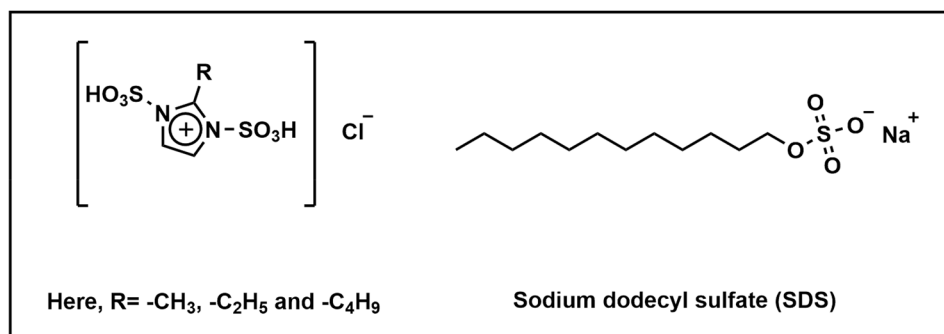
The above-mentioned literature review revealed that there is a scarcity of comparative studies on the effect of Brønsted acidic ILs on the micellization behavior of traditional surfactants. In this study, we explored the aggregation properties of aqueous SDS solution using three members of Brønsted acidic ILs 2-alkyl-1,3-disulfo imidazolium chloride (Fig. 1) containing varied C-2 alkyl group by conductivity, surface tension, and UV–Vis methods at various temperatures and concentrations of the ILs for determination of the CMCs of SDS-IL mixtures. The experimental results of conductivity and surface tension measurements were used to obtain the thermodynamic and surface parameters of the SDS-IL mixtures, respectively. The structural alterations of SDS-IL mixtures were evidenced from their FT-IR spectra. The zeta potential measurement was done to know the stability of colloidal system of SDS-IL mixtures. All these investigations provide a better insight for the type of interactions existing in hydrophobic and hydrophilic part of the surfactant and Brønsted acidic ionic liquids (BAILs).

Materials and methods

Materials

All required chemicals were purchased from chemical suppliers Sisco Research Laboratories Pvt. Ltd, Alfa Aesar, and Tokyo Chemical Industry almost in pure states (97–99%) to synthesize the three ionic liquids. These included 2-methyl imidazole (99%), chlorosulfonic acid (97%), sodium dodecyl sulfate (99%), 2-ethylimidazole (98%), and 2-butylimidazole (>97%). The three $-\text{SO}_3\text{H}$ functionalized ionic liquids of

Fig. 1 Structures of 2-alkyl-1,3-disulfoimidazolium chloride and SDS



2-alkyl-1,3-disulfoimidazolium chloride [RDSIM]Cl, where R = Me-, Et-, and n-Bu- (Fig. 1) were prepared as mentioned in previous literature [30, 49].

Synthesis and characterization of 2-alkyl-1,3-disulfoimidazolium chloride ionic liquids

The three members of 2-alkyl-1,3-disulfoimidazolium chloride ionic liquids [RDSIM]Cl, where R = Me, Et, and n-Bu (Fig. 1), were synthesized as per the standard literature method [49]. Initially, 20 mmol of 2-substituted imidazole was added to dissolve in 10 mL of dry CH₂Cl₂ in a 100-mL two-neck round bottomed flask with stirring for 10 min. Then, chlorosulfonic acid (40 mmol) was added to the stirred solution dropwise under ice cold condition. The reaction mixture was continued to stir for 1 h at room temperature to obtain the [RDSIM]Cl as viscous liquid. The dichloromethane (DCM) solution was removed in rotary evaporator under reduced pressure to isolate the viscous liquid. The crude IL product was washed with dry DCM (3 × 5 mL) and then decanted to get the pure IL, followed by drying in a vacuum oven at 60 °C to remove the trace CH₂Cl₂. The structures of three ionic liquids were further confirmed by taking NMR (¹H and ¹³C) spectra (Figs. S1–S3) in DMSO-d₆ solvent using JEOL400 MHz spectrophotometer and FT-IR spectra with PerkinElmer MIR-FIR FT-IR spectrophotometer. Furthermore, the water contents of ionic liquids were calculated from their TGA (Fig. S4) and TGA-derivative curves (Fig. S5). The first event weight losses in the derivative curves around 70–100 °C show evaporation of the moisture content of ionic liquids. By considering this weight loss as the weight of water, the remaining weight is taken as the weight of ionic liquids to obtain the empirical formulas of ionic liquids (Table S1).

Methods

The micellization properties of SDS were explored in dilute aqueous solutions of ILs. The stock solutions of the three ILs were prepared using Shimadzu BL 220H weighing balance.

The sample solutions were prepared in freshly prepared deionized double distilled water.

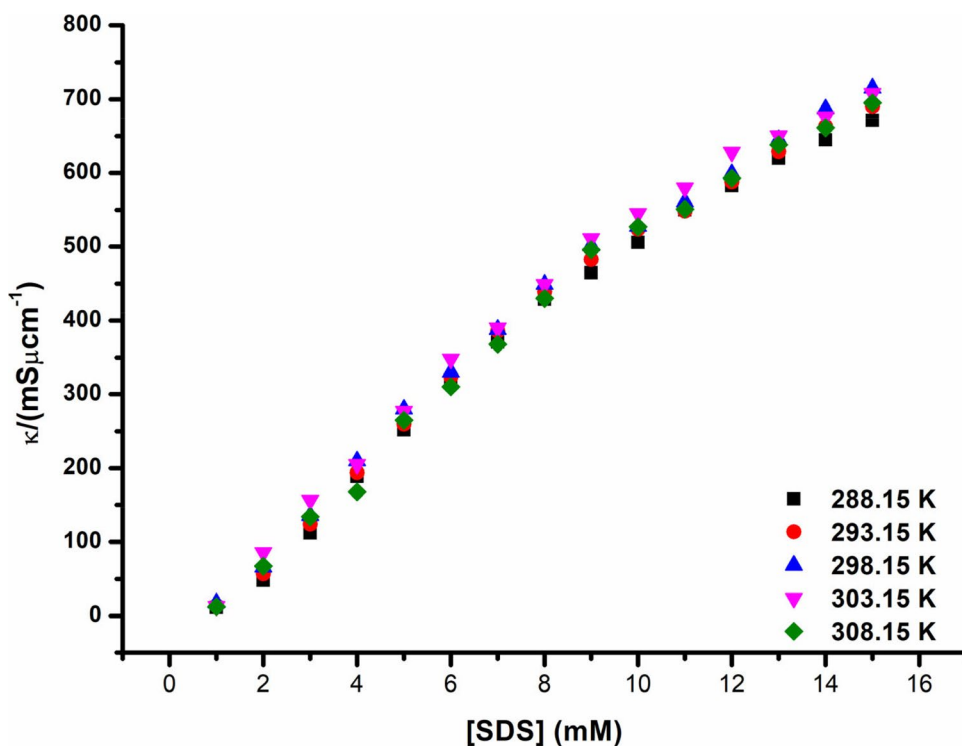
Conductivity measurement

The conductivity of aqueous solution of SDS with or without ILs was determined with Eutech instruments PC 700 Ph/Mv/conductivity/°C/°F/meter. It provides a conductivity range of 0–200 mS and 0–2000 μS. The instrument gives a full-scale resolution of 0.5% and accuracy of ± 1% with the unit cell constant. It has the provision of temperature monitoring facility. The instrument was calibrated using a 0.1 M KCl solution, both before and after the measurements were taken. For determination of the CMC of surfactant-IL solutions, 100 mL of aqueous stock solutions of different concentrations of the ILs (e.g., 0.02, 0.05, 0.08, 0.5, 1, 3, and 5 wt%) were prepared in 100-mL volumetric flask. Then 50 mL of the stock solution of IL was taken in a 100-mL beaker and treated with increasing concentration of SDS with stirring and measured the specific conductance values at different temperatures (288.15 K, 293.15 K, 298.15 K, 303.15 K, and 308.15 K). Each measurement was repeated three times and then average values were taken for analysis. The plots of the conductivity vs. [SDS] showed two linear segments from which the CMC data can be obtained from the point of intersection (Figs. 2 and 3a).

Surface tension measurement

The surface tensions of aqueous SDS/SDS-IL stock solutions of ILs concentrations 0.02, 0.05, and 0.08 wt% were determined with a surface tensiometer (JENCON, India) using a platinum ring by the ring detachment approach. The instrument was calibrated against double distilled water. Before each measurement, the platinum ring was perfectly cleaned and dried. The evaluation was done by dipping the vertically hung ring into the liquid to measure its surface tension. Then, it was pulled out. The maximum force required to draw the ring across the interface was then displayed as the surface tension. Each of the experiments was repeated three times to get the expected surface tension value of water (72

Fig. 2 Specific conductance vs. concentration of aqueous solution of [SDS] at temperatures 288.15 K, 293.15 K, 298.15 K, 303.15 K, and 308.5 K



mNm^{-1}). The results of surface tension values were accurate within $\pm 0.1 \text{ mNm}^{-1}$.

UV–Vis spectroscopy

Shimadzu UV 1800 spectrophotometer was used to record the UV–visible spectra of the IL-SDS solution in the range of 200–800 nm with wavelength accuracy of 0.1 nm. Two quartz cuvette spectrometer cells of 10 mm (3.5 mL) were chosen as reference cell, and measurement cell. Baseline corrections were performed with double-distilled water before the UV analysis. From the conductivity studies, it was decided to choose the aqueous stock solutions of ILs with concentrations 0.02, 0.05, and 0.08 wt % for determination of the CMCs of SDS using UV-method. For this purpose, 100 mL of different concentrations of the stock solutions were prepared in volumetric flask. Then 50 mL of each of the IL solution was treated in a 100-mL beaker with constant increment of SDS concentration with stirring and then kept 3 mL of the SDS-IL solution in the quartz cuvette for analysis. An absorption peak around 260–270 nm was observed for each of the SDS-IL solutions. The CMCs of different SDS-IL solutions were obtained by plotting the graph of absorption intensities against the SDS concentrations. Each one of the observations was repeated three times for confirmation of the data.

FT-IR spectroscopy study

FT-IR spectra of the IL-SDS solutions were obtained from PerkinElmer MIR-FIR FT-IR spectrophotometer in the range of 4000–400 cm^{-1} . Liquid cell (Perkin Elmer; Sl. No. *L1270986*) was utilized in this analysis. The cell consists of two plates of KBr ($l=4 \text{ cm}$ and $b=2 \text{ cm}$) with a spacer size of 4 mm. The liquid sample was placed in between the plates and subjected to analysis. The concentrations of SDS were considered at CMC, below CMC, and above CMC for all the SDS-IL mixtures (0.02, 0.05, and 0.08 wt% of ILs). The wave number accuracy was found within the range of $\pm 0.01 \text{ cm}^{-1}$.

Zeta potential measurement

The zeta potential measurements were done on a zeta sizer (Nano ZS90, Malvern Analytical) with a He–Ne laser equipped with a built-in temperature controller. The accuracy and precision of the Zeta sizer instrument were within 2%. The temperature was kept at 298.15 K for all the analysis. The prepared IL-surfactant solutions of varied concentrations were put in quartz cell during analysis. Repeated measurements were carried out for each of the sample and average data was taken for analysis.

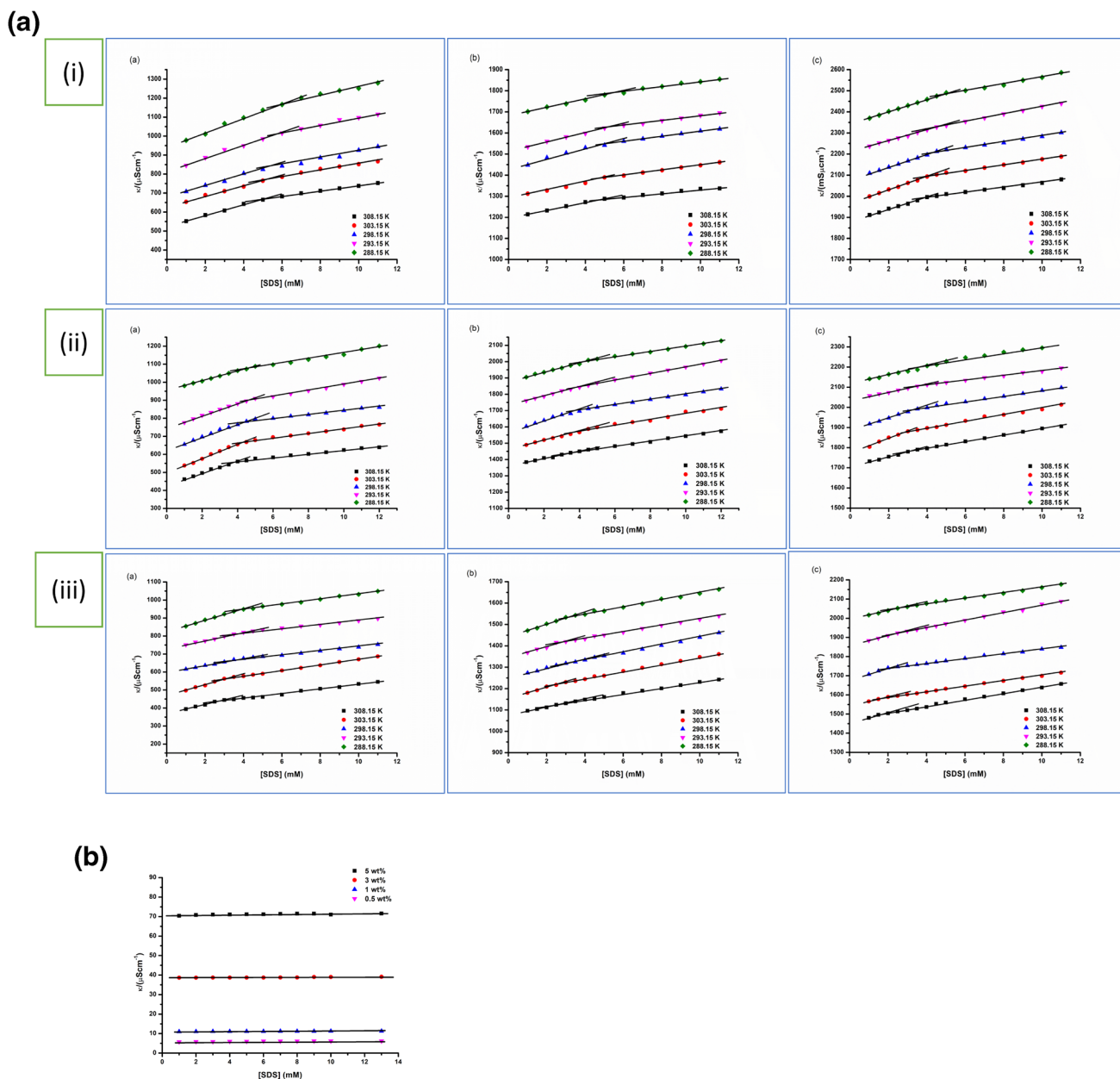


Fig. 3 **a** Specific conductance vs. concentration of [SDS] in **a** 0.02 wt%, **b** 0.05 wt%, and **c** 0.08 wt% of (i) [MDSIM]Cl, (ii) [EDSIM]Cl, and (iii) [BDSIM]Cl at temperatures 288.15 K, 293.15 K, 298.15

K, 303.15 K, and 308.15 K. **b** Specific conductance vs. concentration of [SDS] in 0.5 wt%, 1 wt%, 3 wt%, and 5 wt% of [MDSIM]Cl at 298.15 K

Results and discussions

To study the aggregation behavior of anionic surfactant SDS in aqueous solution of $-\text{SO}_3\text{H}$ functionalized 2-alkyl-1,3-disulfo imidazolium chloride [RDSIM]Cl, where R = Me-, Et-, and n-Bu- (Fig. 1) ionic liquids (ILs) at different concentrations and temperatures, all the three liquids were prepared as per the reported methods [30, 49]. Their structures were

confirmed from spectroscopic data of NMR (^1H and ^{13}C) and FT-IR spectra (Figs. S1–S3). The micellization behaviors of anionic surfactant SDS in aqueous solution of the 2-alkyl 1,3-disulfo imidazolium chloride ILs, i.e., [MDSIM]Cl, [EDSIM]Cl, and [BDSIM]Cl, were studied in different concentrations and temperatures using conductometric measurement, surface tension measurement, and UV–visible spectroscopic techniques [47, 48, 50–53] to understand the effects of

Table 1 CMC value for surfactant (SDS) at various concentrations of [MDSIM][Cl], [EDSIM][Cl], and [BDSIM][Cl] at different temperatures

IL	IL wt%	CMC value at different temperatures (mM)				
		288.15 K	293.15 K	298.15 K	303.15 K	308.15 K
-	0	9.14	8.75	8.20	7.87	7.80
[MDSIM][Cl]	0.02	6.04	5.73	5.56	5.21	5.10
	0.05	5.48	5.13	5.00	4.72	4.60
	0.08	4.82	4.67	4.36	4.01	3.80
[EDSIM][Cl]	0.02	4.85	4.61	4.49	4.27	4.05
	0.05	4.22	3.97	3.70	3.61	3.50
	0.08	3.63	3.39	3.25	2.91	2.77
[BDSIM][Cl]	0.02	3.85	3.63	3.36	2.92	2.80
	0.05	3.14	2.85	2.62	2.49	2.25
	0.08	2.57	2.32	1.94	1.76	1.65

Standard uncertainties s are 0.008–0.009

ILs in the micellization process. The uncertainties associated with the data of micellization studies were mentioned with the table without knowing their exact sources.

In this context, we examined the conductivities of three stock solutions of the ionic liquids at lower concentrations (0.02, 0.05, and 0.08 wt%) at five different temperatures (288.15 K, 293.15 K, 298.15 K, 303.15 K, and 308.15 K). This conductivity measurement expressed the minimum amount of IL need to reduce the CMCs of SDS in these SDS-IL solutions. After that, the concentration of one representative ionic liquid [MDSIM]Cl was increased (0.05, 1, 3, and 5 wt%) and measured their conductivities at 298.15 K to observe the effects of higher amount of IL in the micellization process. From the results of conductometric method, the minimum concentrations of ILs were considered to prepare the stock solutions for determination of the CMCs of SDS using the surface tension and UV–vis techniques at 298.15 K for comparative studies.

Conductivity measurements

Determination of degree of dissociation constant (α), critical micelle concentration (CMC), and thermodynamic parameters

Conductivity assessment can be utilized for characterization of ionic surfactant due to different ionic mobilities of individual ions and their aggregates in aqueous solution. The conductivities of aqueous solution of SDS were measured with or without presence of the ILs, i.e., [MDSIM][Cl], [EDSIM]Cl, and [BDSIM][Cl], to study their effects on the aggregation behavior of SDS at various concentrations and temperatures.

The conductivity vs. concentration of SDS plots of aqueous SDS solutions (Table S2 and Fig. 2) and the aqueous SDS-IL

solutions with lower concentration (0.02, 0.05, and 0.08 wt%) of the ILs were represented in Fig. 3a (Tables S3–S5), respectively, at five temperatures (288.15 K, 293.15 K, 298.15 K, 303.15 K, and 308.15 K). It was seen that the value of conductivity rises with increase in surfactant concentration until the micelle formation takes place after which the rate of conductivity decreases. Two distinguished linear regions were found in the plots, and calculating the ratios of slopes obtained from these plots helped us to determine the value of degree of counter ion dissociation (α) [48, 54].

$$\alpha = S_2/S_1 \quad (1)$$

where S_2 = slope of post micellar region and S_1 = slope of pre-micellar region.

In this study, the slope of conductivity curve in pre-micellar region is found to be higher than the post-micellar region. This reflects that charge carriers become fewer above the CMC than the concentration of surfactant added. The decreasing slope of conductivity above the CMC can be attributed for binding of some counterions to the surface of micelles which reduces the effective charge and thus slower the mobility of aggregates. The degree of counterion binding to micelle (β) can be calculated from the degree of dissociation of counterion (α), as $\beta = (1 - \alpha)$ which indicates the number of anions on the surface of micelles. The conductivity results in Table 1 express that at a particular temperature, the degree of counterion binding values decreases with increasing wt% of the acidic ILs except few observations. The CMC values of SDS for all the lower concentration aqueous SDS-IL solutions were calculated from the point of intersection of specific conductivity vs. SDS concentration plots (Fig. 3a) and included in Table 1 and 2 under the studied temperatures. The observed CMC values follow a decreasing trend with increasing amount of the Brønsted acidic ILs in the mixed SDS-IL solutions and rise of temperature at a particular concentration of ILs. The

Table 2 Thermodynamic parameters of micellization of SDS in different wt% of ionic liquids [MDSIM]Cl (A), [EDSIM]Cl (B), and [BDSIM]Cl (C) at temperatures 288.15 K, 293.15 K, 298.15 K, 303.15 K, and 308.15 K

A Thermodynamic parameters of micellization of SDS in presence of [MDSIM]Cl						
[MDSIM]Cl (wt%)	CMC (mM)	α	β	ΔG_m° (kJ·mol ⁻¹)	ΔH_m° (kJ·mol ⁻¹)	ΔS_m° (J·mol ⁻¹ ·K ⁻¹)
<i>T</i> = 288.15 K						
0	9.14	0.45	0.55	-0.41	1.08	5.01
0.02	6.04	0.46	0.54	-0.43	2.33	9.58
0.05	5.48	0.65	0.35	-0.93	2.42	11.63
0.08	4.82	0.51	0.41	-1.67	4.12	20.10
<i>T</i> = 293.15 K						
0	8.75	0.49	0.51	-0.42	1.046	5.00
0.02	5.73	0.51	0.49	-0.46	2.34	9.55
0.05	5.13	0.56	0.44	-1.05	2.67	12.69
0.08	4.67	0.57	0.43	-1.67	4.08	19.62
<i>T</i> = 298.15 K						
0	8.20	0.54	0.46	-0.44	0.97	4.87
0.02	5.56	0.58	0.42	-0.45	2.30	9.23
0.05	5.00	0.51	0.49	-1.16	2.86	13.48
0.08	4.36	0.59	0.41	-1.75	4.16	19.83
<i>T</i> = 303.15 K						
0	7.87	0.57	0.43	-0.43	0.92	4.65
0.02	5.21	0.59	0.41	-0.49	2.36	9.40
0.05	4.72	0.77	0.23	-1.02	2.44	11.42
0.08	4.01	0.73	0.27	-1.69	3.88	18.38
<i>T</i> = 308.15 K						
0	7.80	0.58	0.42	-0.51	0.89	4.54
0.02	5.10	0.60	0.40	-0.30	2.86	9.76
0.05	4.61	0.68	0.32	-0.34	3.14	11.16
0.08	3.82	0.74	0.26	-0.54	4.79	17.29

Table 2 (continued)

B Thermodynamic parameters of micellization of SDS in presence of [EDSIM]Cl

[EDSIM]Cl (wt%)	CMC (mM)	α	β	ΔG_m^o (kJ·mol ⁻¹)	ΔH_m^o (kJ·mol ⁻¹)	ΔS_m^o (J·mol ⁻¹ ·K ⁻¹)
<i>T</i> = 288.15 K						
0	9.14	0.45	0.54	-0.41	1.08	5.01
0.02	4.85	0.44	0.55	-0.49	1.29	6.18
0.05	4.22	0.53	0.46	-1.19	2.93	14.30
0.08	3.63	0.61	0.38	-1.86	3.62	19.02
<i>T</i> = 293.15 K						
0	8.75	0.49	0.51	-0.42	1.046	5.00
0.02	4.61	0.54	0.46	-0.50	1.25	5.97
0.05	3.97	0.50	0.50	-1.30	3.09	14.98
0.08	3.39	0.66	0.34	-1.94	3.61	18.94
<i>T</i> = 298.15 K						
0	8.20	0.53	0.46	-0.43	0.97	4.87
0.02	4.49	0.53	0.47	-0.52	1.30	6.12
0.05	3.70	0.48	0.52	-1.43	3.24	15.67
0.08	3.25	0.65	0.35	-2.05	3.77	19.53
<i>T</i> = 303.15 K						
0	7.87	0.57	0.43	-0.43	0.92	4.65
0.02	4.27	0.68	0.32	-0.49	1.21	5.61
0.05	3.61	0.70	0.30	-1.27	2.87	13.66
0.08	2.91	0.69	0.31	-2.02	3.77	19.11
<i>T</i> = 308.15 K						
0	7.80	0.58	0.42	-0.51	0.89	4.54
0.02	4.05	0.60	0.40	-0.31	1.49	5.84
0.05	3.50	0.70	0.30	-0.47	3.18	11.84
0.08	2.77	0.72	0.28	-1.98	3.53	17.88

Table 2 (continued)

C Thermodynamic parameters of micellization of SDS in presence of [BDSIM]Cl

[BDSIM]Cl (wt%)	CMC (mM)	α	β	ΔG_m^0 (kJ·mol ⁻¹)	ΔH_m^0 (kJ·mol ⁻¹)	ΔS_m^0 (J·mol ⁻¹ ·K ⁻¹)
<i>T</i> = 288.15 K						
0	9.14	0.45	0.56	-0.41	1.08	5.01
0.02	3.85	0.43	0.57	-0.57	2.59	10.97
0.05	3.14	0.49	0.51	-1.46	7.91	32.53
0.08	2.57	0.50	0.50	-2.45	18.20	71.70
<i>T</i> = 293.15 K						
0	8.75	0.49	0.51	-0.42	1.046	5.00
0.02	3.63	0.43	0.53	-0.61	2.69	11.26
0.05	2.85	0.50	0.50	-1.60	8.14	33.24
0.08	2.32	0.63	0.37	-2.47	17.21	67.16
<i>T</i> = 298.15 K						
0	8.20	0.54	0.46	-0.43	0.97	4.87
0.02	3.36	0.62	0.38	-0.59	2.45	10.20
0.05	2.62	0.63	0.37	-1.62	7.68	31.21
0.08	1.94	0.64	0.36	-2.79	17.67	68.65
<i>T</i> = 303.15 K						
0	7.87	0.57	0.43	-0.43	0.92	4.65
0.02	2.92	0.56	0.44	-0.70	2.64	11.02
0.05	2.49	0.60	0.40	-1.75	8.12	32.57
0.08	1.76	0.65	0.35	-3.05	18.14	69.93
<i>T</i> = 308.15 K						
0	7.80	0.58	0.42	-0.51	0.89	4.54
0.02	2.80	0.64	0.36	-0.65	2.40	9.89
0.05	2.25	0.66	0.34	-1.51	7.99	30.83
0.08	1.65	0.68	0.32	-3.70	16.41	65.26

Standard uncertainties *s* are : *s* (*T*) = ±0.1 K, *s* (CMC) = ±0.0002 mM, *s* (ΔG_m^0) = ±0.02 kJ·mol⁻¹, *s* (ΔH_m^0) = ±0.02 kJ·mol⁻¹, *s* (ΔS_m^0) = ±0.03 J·mol⁻¹·K⁻¹

above trend of reduction of CMC values was further confirmed from linear region of the specific conductivity plots of SDS solutions at higher concentrations (0.5, 1.3, and 5 wt%) of [MDSIM]Cl as an illustrative example in Fig. 3b (Table S6) at 298.15 K.

The observed alteration of CMC values of the SDS-IL solutions can be expected from change of electrostatic interactions occurring between charged head groups as well as hydrophobic interactions of the hydrophobic tails of surfactant, because of temperature, variation of concentration, and alkyl chain length of the ILs to induce the micellization or aggregation behavior of SDS in aqueous solution. The error bars of conductivity measurements of the aqueous SDS solution at 298.15 K and the SDS-IL solutions with lower concentrations (0.02, 0.05, and 0.08 wt%) of IL are included in Figs. 4 and S6, respectively, as typical examples.

Influence of temperature

From Table 1, it could be easily observed that the CMC values of the SDS-IL solutions reduce gradually with rise in temperature. At a particular concentration of the functionalized imidazolium ILs, the rise of temperature may lead to formation of micelles of anionic surfactant at lower concentration through stabilization by adsorption of varied-sized aggregates of the ILs on their surfaces. It was mentioned by Das et al. [30] that the conductivity of Brønsted acidic imidazolium IL solution decreased slowly with increasing temperature which was described due to aggregative nature of these ILs to reduce their excess energy with rise of temperature. This may lead to decrease in hydration process of hydrophilic groups of monomers and thus favors the CMC formation at high temperature and lower concentration of SDS [30].

Influence of concentration of ILs

The increasing concentration of [MDSIM]Cl, [EDSIM]Cl, and [BDSIM]Cl ionic liquids at a particular temperature decreases the CMC values of the surfactant-IL solutions. The presence of Brønsted acidic IL may work for reduction of electrostatic repulsions among the hydrophilic head of SDS monomer by adsorption of constituent ions of IL molecules on the micelle surface through H-bonding interactions involving two N–SO₃H groups of imidazolium cation and thereby increasing the tendency of micellization in aqueous solution resulting to greater decrease of the values of CMC. Another possibility can also be expected by mixing of the BAIL with the SDS solution for conductivity studies involving anion exchange reaction with formation of water soluble NaCl and bi-amphiphilic surface-active ionic

liquids of 2-alkyl-1,3-disulfo imidazolium cation with dodecyl sulfate as counter anion. It was reported that such types of bi-amphiphilic ionic liquids possess low CMC value as compared to their similar alkyl chain length surfactant and ionic liquids [55]. The conductivities of the SDS-IL solutions indicate the need for a minimum amount of the IL to get the CMCs at the lower SDS concentrations. It is also observed that with increasing amount of the ILs in SDS-IL solutions, the CMC values decrease which evidence the formation of bi-amphiphilic surface-active ionic liquids in aqueous solution.

Influence of alkyl chain length of ILs

Alkyl chain tethered to the ILs showed profound effect on the aggregation behavior of the surfactant. The decreasing order of CMC values was found as [BDSIM]Cl < [EDSIM]Cl < [MDSIM]Cl in all the experimental conditions. It implies that longer alkyl chain provides better hydrophobic interactions [56, 57] with water molecules in Fig. 3a which favor the micellization process by making them available for aggregation and thus diminished the CMC values observed.

Thermodynamics of micellization

To understand the thermodynamics of micellization or to calculate various thermodynamic parameters [54, 58], the equilibrium model of micellization should be considered. The micellization of anionic surfactant could be represented as:



where, S⁻ represents anionic surfactant ions, C⁺ is its counterions, and M^{p-} is the aggregates of **n** monomers having effective charge *p*. Standard free energy change per mole of the surfactant is given by

$$\Delta G_m^0 = RT(-1/n \ln a_M^{p-} + \ln a_s^- + (1 - p/n) \ln a_c^+) \quad (3)$$

where *a* stands activity of the species and *n* represents aggregation number. If *n* ≥ 50, i.e., *n* is large the first term becomes negligibly small and *a_s⁻* and *a_c⁺* could be replaced by activity at the CMC. Since the CMC occurs at dilute solutions so activity could be replaced by concentration of the surfactant. Considering all these calculations, the standard free energy of micellization could be expressed as [58]

$$\Delta G_m^0 = (2 - \alpha) \cdot RT \ln X_{CMC} \quad (4)$$

Similarly, the standard free energy of micellization could be expressed as

$$\Delta H_m^0 = -RT^2(2 - \alpha) \left[d(\ln X_{CMC}) / dT \right] \tag{5}$$

By using the values of ΔG_m^0 and ΔH_m^0 , the values of ΔS_m^0 is represented as

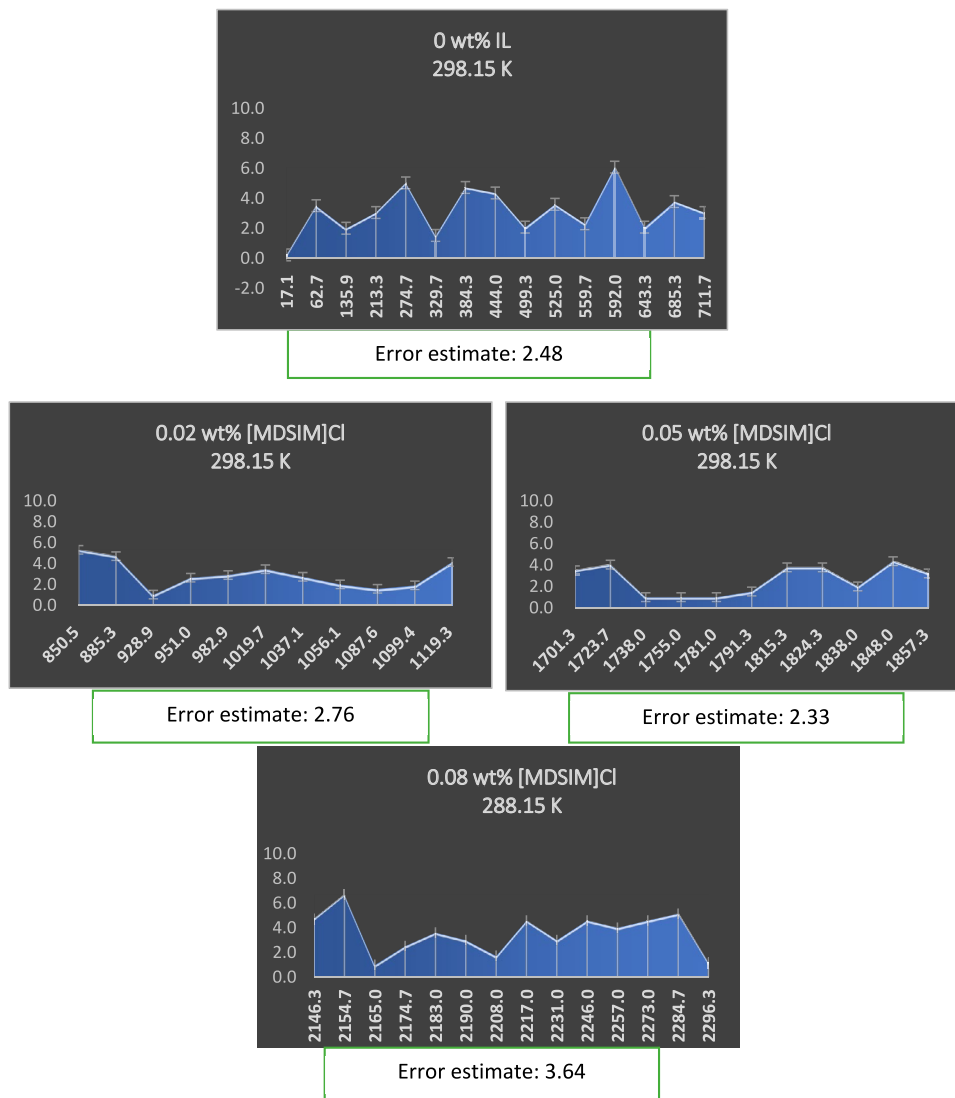
$$\Delta S_m^0 = (\Delta H_m^0 - \Delta G_m^0) / T \tag{6}$$

where R is universal gas constant, T represents temperature, X_{CMC} is the concentration of SDS at CMC in mole fraction unit, and α is degree of counterion dissociation.

The values of various thermodynamic parameters were calculated and included in the three sections of Table 2 (A, B, and C). The negative ΔG_m^0 values for micellization of SDS in water and with ionic liquid–water solutions indicate spontaneous nature of the micellization process in these solutions like earlier report of Kumar et al. [47] using 1-butyl-3-methylimidazolium chloride ionic liquid.

The ΔG_m^0 values of the ILs follow the trend as [BDSIM]Cl > [EDSIM]Cl > [MDSIM]Cl for all the concentrations of ILs and temperatures which could be attributed to decrease in alkyl chain length [53]. Thus, the IL with longer hydrophobic group provides more spontaneity to the system. Effect of temperature is also significant in this case. With rise in temperature and concentration of the IL, more negative ΔG_m^0 values are observed which indicate favorable condition of the micellization process. The positive values of ΔH_m^0 express endothermic nature of the micellization process unlike the previous literature [47]. The increased ΔH_m^0 values against rising the concentration of ILs and temperatures represent requirement of more heat to the micellization process. Hydrophobic interactions acted as prime factors for the positive values of ΔH_m^0 in contrast to London-dispersion interactions in case of the negative values of ΔH_m^0 . Standard entropy of micellization values for all the system are found to be small and positive. Very small values of $T\Delta S_m^0$ as compared to the ΔH_m^0 express

Fig. 4 Representative error bars of the conductivity measurements of SDS solution in absence and presence of various concentrations of [MDSIM]Cl at 298.15 K



less entropy driven character of the aggregation process as compared to the literature report [39, 47, 48]. From Eq. (6), one can expect negative entropy values for the ordered micellar structures of SDS in the aqueous SDS-IL solutions with varied concentrations of the ILs at different temperatures. In contrast, the experimental evidence reveals positive ΔS_m^0 for all the SDS-IL solutions at any temperature under this study. The data for entropy of micellization also show slight variation of positive values of ΔS_m^0 at a particular concentration of each of the IL with rising temperature from 288.15 to 308.15 K. These are found to be unusual as there is a gradual decrease of the entropy of micellization with increased temperature. But with increased concentration of IL, the ΔS_m^0 values become more positive and provide information about the existence of more disordered micellar states in the SDS-IL solutions. This noticeable inconsistency can be accounted by considering modifications of the ordered structures of micelles due to increasing disorder of surrounding water molecules/ionic liquids for reorganization around the micelles. This leads to lower degree of organization compared to those solvating individual SDS monomers at the observed temperature [47]. These effects will show positive entropic contribution to the SDS-IL solutions. The ΔS_m^0 values also express effects of varied sizes of 2-alkyl substituent of imidazolium cation of the ILs in the micellization process. Slight variation of the ΔS_m^0 values is observed using [MDSIM]Cl and [EDSIM]Cl ionic liquids. The higher ΔS_m^0 in presence of [BDSIM]Cl ionic liquid

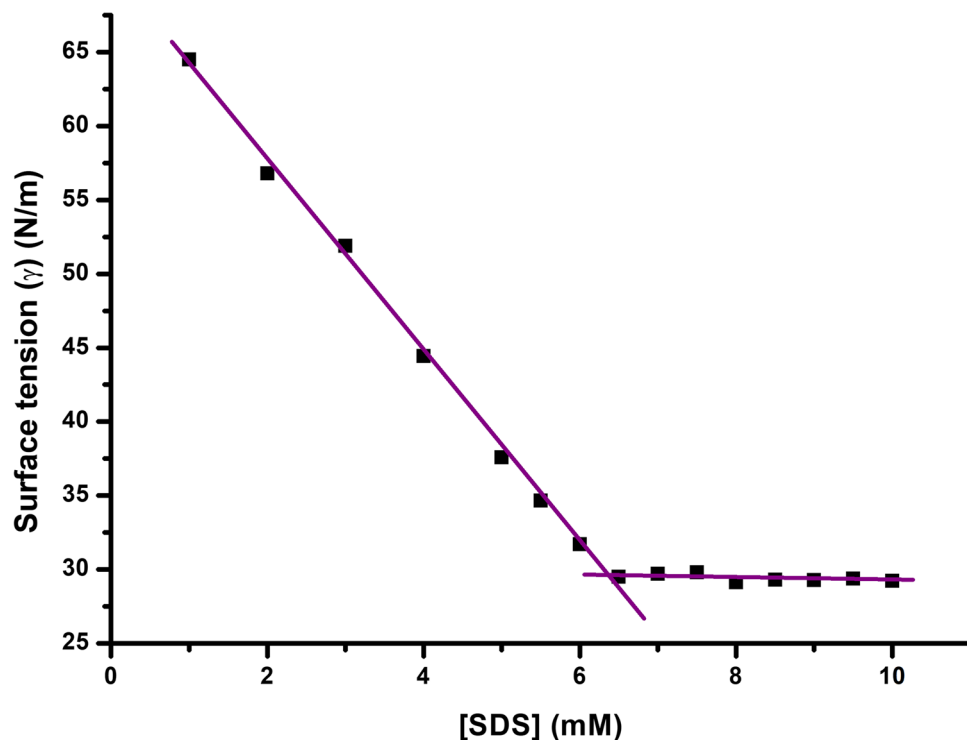
indicate more hydrophobic effect from bulkier 2-nBu group of the imidazolium cation of [BDSIM]Cl in the process of micellization [59].

Surface tension measurement

Determination of surface tension at CMC (γ_{CMC}) and the effect of ionic liquids on interfacial properties

To investigate the surface activity of SDS-IL solutions at varied concentrations of ILs, surface tension measurements were conducted. Figures 5 and 6 show the plots of surface tension (γ) vs. concentration of SDS in absence and presence of the 2-alkyl 1,3-disulfoimidazolium chloride ILs with varied sizes of 2-alkyl group in the concentrations of 0.02, 0.05, and 0.08 wt% of IL at 298.15 K. The surface tension values of the aqueous SDS along with the SDS-IL solutions gradually reduce with increase in the concentration of SDS in solution before achieving a constant value due to saturation of the surface [60]. This point of intersection in these graphs could be taken as the CMC values. The surface tension (γ) value of aqueous SDS solution at the CMC in pure state is 30.06 mN/m and reduction of the γ (CMC) values is observed after mixing with the ILs. Greater reduction of the γ (CMC) values is observed in presence of [BDSIM]Cl ionic liquid which displays better surface activity of the [BDSIM]Cl due to longer 2-nBu substituent of imidazolium cation than the [EDSIM]Cl and [MDSIM]Cl ionic liquids with comparatively smaller 2-alkyl groups.

Fig. 5 Surface tension vs. concentration of SDS in water at 298.15 K



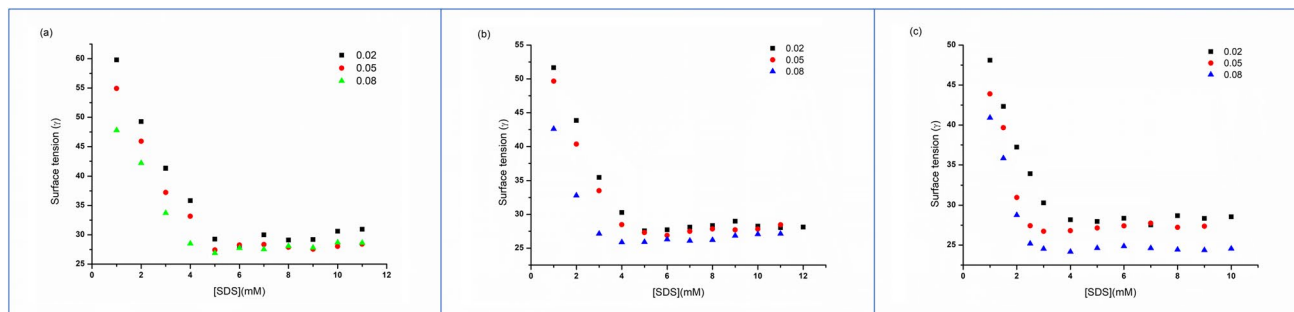


Fig. 6 Surface tension vs. concentration of SDS having 0.02 wt%, 0.05 wt%, and 0.08 wt% of **a** [MDSIM]Cl, **b** [EDSIM]Cl, and **c** [BDSIM]Cl at 298.15 K

Several parameters related to the surface activity of aqueous SDS-IL solutions can be used to get from the plots of surface tension (γ) vs. $\log[\text{SDS}]$ in Fig. 7. The results of surface parameters including surface tension (γ_{CMC}) and surface pressure (π_{CMC}) at the CMC, surface excess concentration (Γ_{max}), minimum surface area per molecule (A_{min}), and packing parameter (P) are shown in Table 3 and 4 as calculated from Eqs. (7)–(13). The surface pressure (π_{CMC}) at the CMC for all the SDS-IL solutions was interpreted by Eq. (7) [61].

$$\pi_{\text{CMC}} = \gamma_o - \gamma_{\text{CMC}} \quad (7)$$

in which γ_o is the surface tension of pure aqueous SDS solution and γ_{CMC} is the measured surface tension at the CMC [62].

Maximum surface excess concentration, minimum area per molecule, and packing parameters

The extent of surfactant adsorption at the surface of a liquid is defined in terms of surface excess concentration. It is the amount of surfactant available per unit area of interface in excess of the amount of surfactant that would be present if uniform concentration existed at that surface. The maximum surface excess concentration (Γ_{max}) was determined by the Gibbs adsorption equation to the surface tension data by Eq. (8) [63–65]:

$$\Gamma_{\text{max}} = -1/2.303nRT \left[dy/d \log C \right] T, P \quad (8)$$

in which T represents absolute temperature, R is molar gas constant, and γ is the surface tension at the CMC. The pre-factor constant “ n ” in the Gibbs equation was assumed to be 2 for the SDS surfactant [66]. In Eq. (8), the slope of changes is calculated from the surface tension isotherm Fig. 7 where, $d\gamma/d\log C$ is the slope of these isotherms and C is the concentration of SDS at CMC of the SDS-IL solutions. The range of data for slope determination was considered those which have adj. r^2 values within 0.95–0.99 along with standard errors ranges 0.08–0.1.

The maximum surface excess concentration (Γ_{max}) of SDS in water was found to be $1.30 \mu\text{mol}/\text{m}^2$ at 298.15 K. Again, the estimated Γ_{max} values of studied SDS-IL solutions are increased with rising concentration of the ILs at 298.15 K which show adsorption of a greater number of the surfactant molecules at the interface with increase of packing density. This tendency is also concurrence with the surface pressure (π_{CMC}) values at the CMC of all the SDS-IL solutions (Table 3).

The minimum area A_{min} ($\text{m}^2\text{mol}^{-1}$) occupied by a single surfactant molecule at the interface of air–water was determined using Eq. (9) [63]:

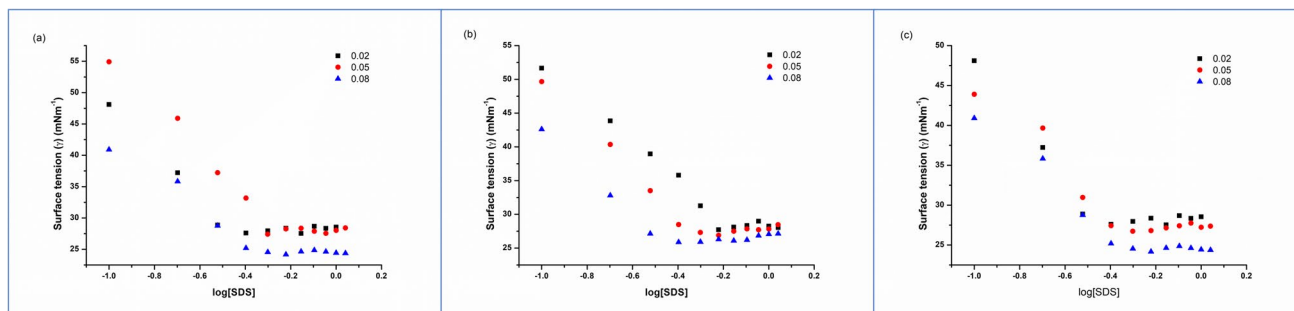


Fig. 7 Surface tension vs. $\log[\text{SDS}]$ having 0.02 wt%, 0.05 wt%, and 0.08 wt% of **a** [MDSIM]Cl, **b** [EDSIM]Cl, and **c** [BDSIM]Cl at 298.15 K

Table 3 CMC, γ_{CMC} , π_{CMC} , Γ_{max} , and A_{min} data of SDS in (0.02, 0.05, and 0.08 wt%) of (i) [MDSIM]Cl (ii) [EDSIM]Cl, and (iii) [BDSIM]Cl

A Surface parameters of micellization of SDS in presence of [MDSIM]Cl					
[MDSIM]Cl wt%	CMC (mM)	γ_{CMC} (mN/m)	π_{CMC} (mN m ⁻¹)	Γ_{max} ($\mu\text{mol}/\text{m}^2$)	A_{min} (\AA^2)
0.00	6.30	29.60	41.00	1.3	127.7
0.02	5.20	28.11	42.49	1.55	107.12
0.05	4.70	27.58	43.02	1.65	100.62
0.08	4.30	26.84	43.76	2.16	76.81
B Surface parameters of micellization of SDS in presence of [EDSIM]Cl					
[EDSIM]Cl wt%	CMC (mM)	γ_{CMC} (mN/m)	π_{CMC} (mN m ⁻¹)	Γ_{max} ($\mu\text{mol}/\text{m}^2$)	A_{min} (\AA^2)
0.00	6.30	29.60	41.00	1.3	127.7
0.02	4.32	27.96	42.64	1.92	86.84
0.05	3.65	26.83	43.77	2.03	81.64
0.08	3.06	25.45	45.15	2.22	74.80
C Surface parameters of micellization of SDS in presence of [BDSIM]Cl					
[BDSIM]Cl wt%	CMC (mM)	γ_{CMC} (mN/m)	π_{CMC} (mN m ⁻¹)	Γ_{max} ($\mu\text{mol}/\text{m}^2$)	A_{min} (\AA^2)
0.00	6.30	29.60	41.00	1.3	127.7
0.02	3.10	27.56	43.04	2.07	80.23
0.05	2.40	26.23	44.37	2.38	69.70
0.08	2.10	24.44	46.16	2.42	68.62

Standard uncertainties s are CMC = 0.007; γ_{CMC} = 0.055; π_{CMC} = 0.002; Γ_{max} = 0.006; A_{min} = 0.009

$$A_{\text{min}} = l/N_A \Gamma_{\text{max}} \quad (9)$$

in which N_A is the Avogadro's number ($6.023 \times 10^{23} \text{ mol}^{-1}$) and Γ_{max} in mol m^{-2} . The minimum surface area A_{min} of all the aqueous SDS-IL solutions (Table 3) expresses decreasing trend for each of the IL with increasing concentration of the IL from 0.02 to 0.08 wt% [64]. The obtained values of A_{min} were used to determine the packing parameters (P) that demonstrate the micellar geometry of the systems predicted by Eq. (10) [67]:

$$P = V_0/l_c A \quad (10)$$

in which V_0 denotes the volume occupied by the hydrophobic portion of alkyl chain length in micellar core, and l_c and A denote the maximum effective length of hydrophobic tail of a monomer and surface area of headgroup of surfactant monomer, respectively. Both the l_c and V_0 of a saturated hydrocarbon chain of carbon number C_n could be obtained using Tanford formula (Eqs. 11 and 12) [67–69]:

$$V_0 = [27.4 + 26.9 C_n] 10^{-3} \text{ nm}^3 \quad (11)$$

$$l_c = [0.154 + 0.1265 C_n] \text{ nm} \quad (12)$$

where C_n is the number of carbon atom in a single hydrophobic chain. Exact measurement of the headgroup area of the micellar surface is quite difficult. So, A_{min} value obtained from the plots of surface tension replaced A for further calculations [70]. For binary mixed surfactant systems, the modified Israelachvili Eq. (13) was used as shown [71]:

$$P_{\text{eff}} = \left[\frac{V_0}{l_c A_{\text{min}}} \right]_{\text{eff}} = \frac{\sum V_i X_i}{(\sum A_i X_i) l_c} \quad (13)$$

For all the stoichiometric mole fractions (X_i) of the mixtures of SDS and ionic liquids, the value of l_c is taken as the number of carbon atom attached to the hydrophobic chains of the ILs. A_{min} values of the individual components of SDS and ILs replace A_i . The calculated values of the P are displayed in Table 4. The critical packing parameter (CPP) theory suggested that when $P \leq 0.333$, the surfactant system forms small micelles, when $1/2 < P \leq 1$, vesicle or bilayer exist and for inverted structures, $P > 1$. From Table 4, it could be concluded that for all the systems of SDS and ILs, $P < 0.333$, which indicate the small spherical shape of the mixtures.

Table 4 Packing parameter (P) values of mixtures of SDS and ionic liquids (a) [MDSIM]Cl, (b) [EDSIM]Cl, and (c) [BDSIM]Cl

Ionic liquid	Wt%	CPP (P)
(a) [MDSIM]Cl	0.02	0.00176
	0.05	0.00177
	0.08	0.00179
(b) [EDSIM]Cl	0.02	0.00207
	0.05	0.00202
	0.08	0.00205
(c) [BDSIM]Cl	0.02	0.00222
	0.05	0.00230
	0.08	0.00225

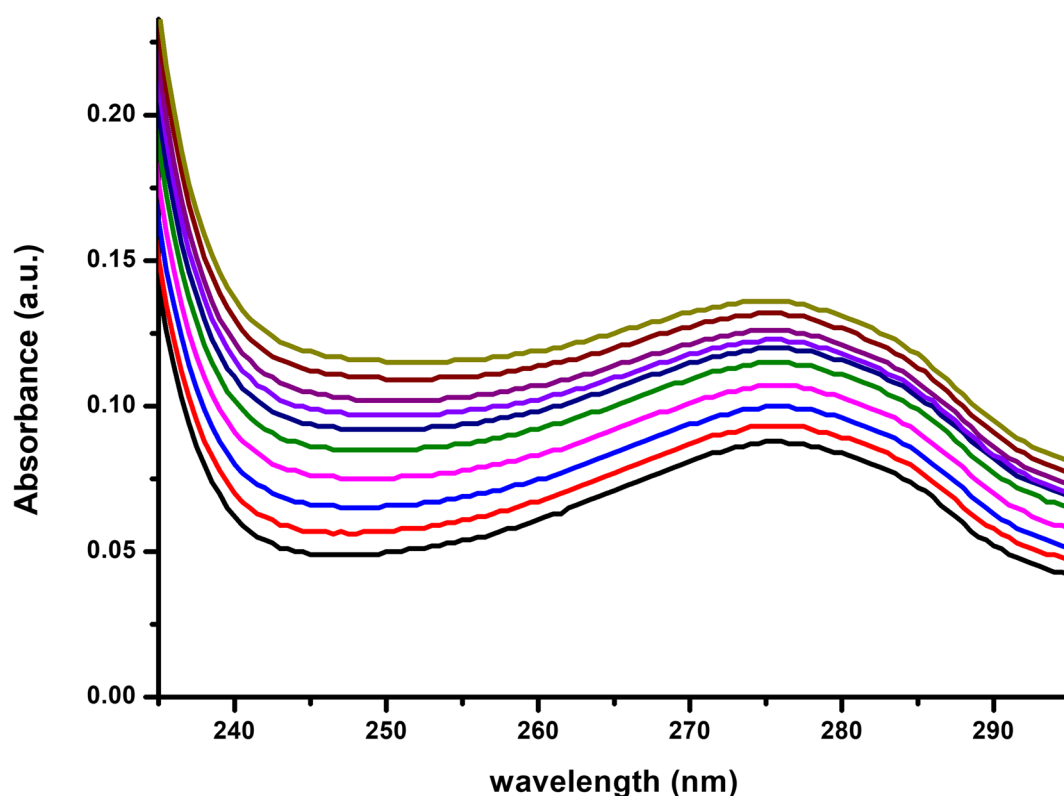
UV–Vis spectroscopic studies

Absorbance behavior of the SDS in aqueous ionic liquid solutions was investigated in UV–Vis range (200–800 nm) at 298.15 K. Presence of imidazole moiety helped the ILs to get absorption in the UV–Vis range and that eliminated the requirement of any kind of probe molecule for the CMC measurement. Concentrations of the solutions rise with the successive addition of SDS solution using the

micropipette. From Fig. 8, it could be observed that the intensity of absorption lines increases up to a certain value and after that the rate becomes slower. This phenomenon could be observed clearly after plotting the absorbance vs. [SDS] graphs (Figs. 9, 10, and 11) having (a) 0.02, (b) 0.05, and (c) 0.08 wt% of the three ILs. These graphs also help to determine the CMC values of the respective SDS-IL systems. From these plots, we get two intersecting lines, and the meeting point of these lines gives us the values of CMC. The rates of increase in absorbance of the two lines are different. The CMC values of the three ILs obtained through the UV–Visible method at 298.15 K were compared to the CMC values of conductivity and surface tension techniques and found that all the values obtained through these methods are close to each other in Table 5 at all concentration of the ionic liquids.

FT-IR spectroscopic analysis

The surfactant-IL systems for all concentrations of the ionic liquids and SDS were subjected for FT-IR analysis to get information of molecular level interactions at the CMC, below, and above the CMC for each of the surfactant-IL systems (Figs. S7–S10). The FT-IR spectra of aqueous SDS solution possess peaks at $3444\text{--}3447\text{ cm}^{-1}$ for O–H stretching

**Fig. 8** Absorbance vs. wavelength plot of SDS in presence of 0.02 wt% of [MDSIM]Cl

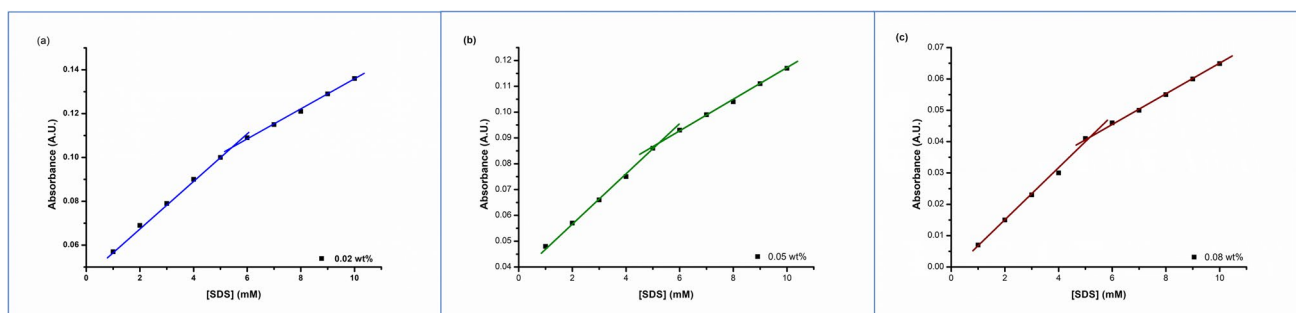


Fig. 9 Variation of absorbance with concentration of SDS in water in the presence of **a** 0.02 wt%, **b** 0.05 wt%, and **c** 0.08 wt% of [MDSIM]Cl at 245 nm

vibration, C–H stretching at $2847\text{--}2860\text{ cm}^{-1}$ and 2912 cm^{-1} , S=O stretching at 1387 cm^{-1} , and C–O stretching at 1019 cm^{-1} [47] in addition to bending vibration of hydrogen bonded water at 1619 cm^{-1} [72]. The FT-IR spectra of all the SDS-IL systems (Figs. S7–S10) display significant change of the peak positions of SDS with intensities in these regions, which imply structural change of the aqueous SDS solution through interactions with the ionic liquid molecules. The peak intensities of O–H stretching vibrations varied in the range $3440\text{--}3450\text{ cm}^{-1}$ due to weakening or breaking of H-bonding

interactions of water molecules with SDS and ionic liquids during the micellization process. The reorganization of water molecules surrounding the aggregates of SDS-IL system may affect the bending vibration of hydrogen-bonded water molecules that appeared near $1621\text{--}1687\text{ cm}^{-1}$ for all the SDS-IL system along with overlapped C=C stretching vibration of the imidazolium cation. As compared to the IR spectra of SDS solution, the fingerprint region peaks also changed differently with intensities for the three ionic liquids, which indicate the effects of ionic liquids in the micellization of SDS.

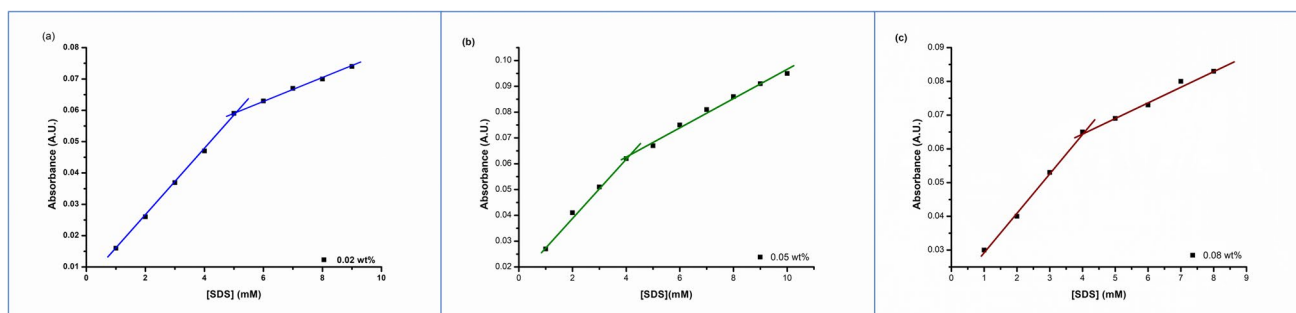


Fig. 10 Variation of absorbance with concentration of SDS in water in the presence of **a** 0.02 wt%, **b** 0.05 wt%, and **c** 0.08 wt% of [EDSIM]Cl at 245 nm

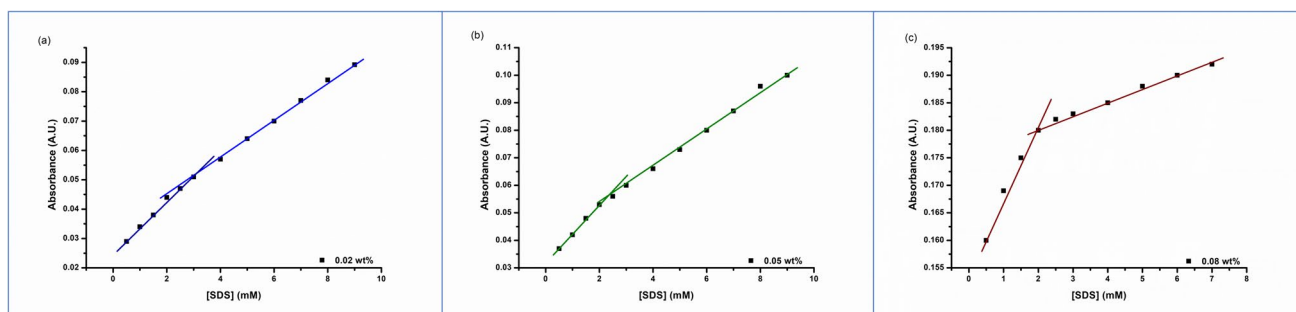


Fig. 11 Variation of absorbance with concentration of SDS in water in the presence of **a** 0.02 wt%, **b** 0.05 wt%, and **c** 0.08 wt% of [BDSIM]Cl at 245 nm

Table 5 Comparative CMC values of SDS in aqueous solution of the SDS-IL systems determined via conductivity, surface tension, and UV–Vis methods**A** CMC of SDS with varied concentration of [MDSIM]Cl

[MDSIM]Cl (wt%)	CMC (mM)		
	Conductivity	Surface tension	UV–Vis Spectroscopy
0.02	5.56	5.20	5.47
0.05	5.00	4.70	5.23
0.08	4.36	4.31	5.12

B CMC of SDS with varied concentration of [EDSIM]Cl

[EDSIM]Cl (wt%)	CMC (mM)		
	Conductivity	Surface tension	UV–Vis Spectroscopy
0.02	4.49	4.32	5.02
0.05	3.70	3.65	4.19
0.08	3.25	3.06	4.03

C CMC of SDS with varied concentration of [BDSIM]Cl

[BDSIM]Cl (wt%)	CMC (mM)		
	Conductivity	Surface tension	UV–Vis Spectroscopy
0.02	3.36	3.10	2.91
0.05	2.62	2.40	2.36
0.08	1.94	2.10	2.06

Standard uncertainties s are conductivity = 0.006; surface tension = 0.008; UV–Vis = 0.007

Zeta potential measurement

Zeta potential is a measurement of electrostatic attraction or repulsion between particles and can be used as a tool to determine the stability of colloidal systems. According to literatures, zeta potential values higher than ± 30 mv are considered to possess sufficient repulsive forces to attain pleasant physical colloidal stability [73]. However, if the particles have too low zeta potential, then there will be no force to prevent them to coming together for flocculation. The negative or positive values of zeta potential display existence of negatively or positively charged surfaces of disperse particles, respectively, in aqueous media which depend on pH of the sample solutions. The zeta potential values of all the studied systems were found to be negative in Table 6 and Fig. S11 and thus confirm the dispersion of negatively charged surfactant molecules in ionic liquid-SDS aqueous media in all the concentrations.

From Table 6, it is seen that the zeta potential values become more negative slowly with rise in concentration of acidic ionic liquid from 0.02 to 0.08 wt% which provide

information about increasing stability of the surfactant-IL aqueous solutions. As the sizes of 2-alkyl group of imidazolium cation increase from Me < Et < n-Bu, then the measured comparative zeta potential values also followed lowering of more negative values in the same order of 2-alkyl group sizes, which follows the ascending order of zeta potential values as [BDSIM]Cl < [EDSIM]Cl < [MDSIM]Cl. This

Table 6 Zeta potential values of SDS with varied concentrations of (a) [MDSIM]Cl, (b) [EDSIM]Cl, and (c) [BDSIM]Cl

Name of IL	Wt % of IL	Zeta potential value (mv)
(a) [MDSIM]Cl	0.02	−16.1
	0.05	−21.3
	0.08	−21.4
(b) [EDSIM]Cl	0.02	−21.5
	0.05	−22.4
	0.08	−25.0
(c) [BDSIM]Cl	0.02	−28.0
	0.05	−29.6
	0.08	−30.5

observation showed SDS-[BDSIM]Cl mixtures are the most stable surfactant-IL system among all the mixtures. This can be attributed for descending order of Brønsted acidic strength as reported earlier for the 1,3-disulfo-2-alkyl imidazolium chloride ionic liquids with increasing sizes of 2-alkyl groups due to positive inductive effect (+I) [30].

Conclusions

In summary, the aggregation behavior of SDS in aqueous solutions was investigated in the presence of three members of $-\text{NSO}_3\text{H}$ functionalized Brønsted acidic IL 2-alkyl-1,3-disulfo imidazolium chloride with increasing sizes of C-2 alkyl group at different temperatures and concentrations of the ILs by employing conductometric, surface tension, and UV–Vis techniques as well as FT-IR analysis of the SDS-IL solutions. The presence of varied concentrations of the acidic ILs significantly affected the CMCs of pure aqueous SDS solution along with alteration of thermodynamic and surface parameters in the SDS-IL solutions. With the increase of IL concentrations for all the solutions, the decreasing trend of CMCs was observed which reflect favorable electrostatic interactions between the IL and SDS molecules toward the micellization process in aqueous media. Among the three ILs with different sized 2-alkyl group of imidazolium cations, minimum CMC values were found for the [BDSIM]Cl because of the more hydrophobic longer alkyl chain of n-butyl substituent. The ascending trend of CMCs of the three ILs was found as [BDSIM]Cl < [EDSIM]Cl < [MDSIM]Cl. At a particular concentration of the IL, the CMCs of SDS solutions were slightly varied within the studied temperatures for all the ILs. This can be accounted for involvement of strong H-bonding and other electrostatic interactions between the sulfonic acid functionalized IL and the SDS surfactant in aqueous media which may be little effected by the rise of temperature from 288.15 to 308.15 K. Negative free energy of micellization (ΔG_m^0) indicates feasibility of the process of micellization. Positive values of enthalpy show the endothermic nature of aggregation. Likewise positive entropy values express modification of the micelle structures because of rising disorder of water/ionic liquid molecules surrounding the micelles for reorganization within the temperature of observations. The surface parameters of SDS-IL solution show that the addition of ILs remarkably declines the surface tension values of the mixtures. The results of surface excess values (Γ_{max}) display more adsorption of surfactant molecules in the interface with larger 2-alkyl group containing [BDSIM]Cl ionic liquid for its higher hydrophobic interactions as compared to the [MDSIM]Cl and [EDSIM]Cl. Subsequently, these outcomes are corroborated with their

descending order of minimum surface area per molecule (A_{min}) values: [BDSIM]Cl > [EDSIM]Cl > [MDSIM]Cl. The critical packing parameter data indicated formation of small spherical structures micellar for all the SDS-IL mixtures. The CMCs estimated using the three methods are in good agreement with each other. FT-IR analyses of the SDS-IL solutions support the change of characteristics of SDS vibrational frequencies in the mixtures. The investigation of zeta-potential reveals gradual improvement of the stability of micellar systems with increasing bulkiness of the C-2-alkyl group of imidazolium cation of ionic liquid. In future, these studies can be extended to observe the micellization behavior of varied types of cationic/anionic surfactants with various Brønsted acidic ionic liquids.

Supplementary Information The online version contains supplementary material available at <https://doi.org/10.1007/s00396-024-05247-w>.

Acknowledgements The authors are thankful to Sophisticated Analytical Instrumentation Centre, Tezpur University, for providing various facilities to carry out experimental works and University Grants Commission (UGC) for providing Senior Research Fellowship to Debanga Bhusan Bora.

Author contribution D.B. B. and R. B. wrote the main manuscript text. All the prime experiments were performed by D. B. B. and B. R. B. The analysis and interpretation of experimental data were done by R.B. and D.B.B. The other co-authors S.P., S. K., and N. K. synthesized and characterized the required ionic liquids. Validation experiments were conducted by S.P., S. K., and N. K. The corresponding author R.B. initiated the original idea of manuscript and supervised the work. All authors approved the final version of manuscript.

Data availability The authors declare that the data supporting the findings of this study are available within the paper and its supplementary information file.

Declarations

Ethical approval Not applicable.

Conflict of interest The authors declare no competing interests.

References

- Lombardo D, Kiselev MA, Magazù S, Calandra P (2015) Amphiphiles self-assembly: basic concepts and future perspectives of supramolecular approaches. *Advances in Condensed Matter Physics* 2015:1–22, Article ID 151683. <https://doi.org/10.1155/2015/151683>
- Panda A, Kumar A, Mishra S, Mohapatra SS (2020) Soapnut: a replacement of synthetic surfactant for cosmetic and biomedical applications. *Sustainable Chemistry and Pharmacy* 17:100297. <https://doi.org/10.1016/j.scp.2020.100297>
- Abbot V, Paliwal D, Sharma A, Sharma P (2022) A review on the physicochemical and biological applications of biosurfactants in

- biotechnology and pharmaceuticals. *Heliyon* 8:e10149. <https://doi.org/10.1016/j.heliyon.2022.e10149>
4. Kralova I, Sjöblom J (2009) Surfactants used in food industry: a review. *J Dispersion Sci Technol* 30:1363–1383. <https://doi.org/10.1080/01932690902735561>
 5. Sun J, Zhang Y, Pan X, Zhu G (2018) The effects of anionic and non-ionic surfactant on anaerobic co-digestion of sludge, food wastes and green wastes. *Environ Technol* 40:2538–2547. <https://doi.org/10.1080/09593330.2018.1446457>
 6. Le Guenic S, Chaveriat L, Lequart V, Joly N, Martin P (2019) Renewable surfactants for biochemical applications and nanotechnology. *J Surfactants Deterg* 22:5–21. <https://doi.org/10.1002/jdsd.12216>
 7. Pan A, Rakshit S, Sahu S, Bhattacharya SC, Moulik SP (2015) Synergism between anionic double tail and zwitterionic single tail surfactants in the formation of mixed micelles and vesicles, and use of the micelle templates for the synthesis of nano-structured gold particles. *Colloids Surf A* 481:644–654. <https://doi.org/10.1016/j.colsurfa.2015.06.032>
 8. Mukherjee I, Dinda G, Ghosh S, Moulik SP (2012) Synthesis, characterization, and applications of microheterogeneous-templated CdS nanodispersions. *J Nanopart Res* 14:1–4. <https://doi.org/10.1007/s11051-012-0997-z>
 9. Quintero L (2002) An overview of surfactant applications in drilling fluids for the petroleum industry. *J Dispersion Sci Technol* 23:393–404. <https://doi.org/10.1080/01932690208984212>
 10. Zhou C, Wang D, Cao M, Chen Y, Liu Z, Wu C, Xu H, Wang S, Wang Y (2016) Self-aggregation, antibacterial activity, and mildness of cyclodextrin/cationic trimeric surfactant complexes. *ACS Appl Mater Interfaces* 8:30811–30823. <https://doi.org/10.1021/acsami.6b11667>
 11. Liu K, Yang L, Peng X, Wang J, Lu JR, Xu H (2020) Modulation of antimicrobial peptide conformation and aggregation by terminal lipidation and surfactants. *Langmuir* 36:1737–1744. <https://doi.org/10.1021/acs.langmuir.9b03774>
 12. Oremusová J, Vitková Z, Vitko A, Tárník M, Miklovičová E, Ivánková O, Murgaš J, Krchňák D (2019) Effect of molecular composition of head group and temperature on micellar properties of ionic surfactants with C12 alkyl chain. *Molecules* 24:651. <https://doi.org/10.3390/molecules24030651>
 13. Davies TS, Ketner AM, Raghavan SR (2006) Self-assembly of surfactant vesicles that transform into viscoelastic wormlike micelles upon heating. *J Am Chem Soc* 128:6669–6675. <https://doi.org/10.1021/ja060021e>
 14. Svenson S (2004) Controlling surfactant self-assembly. *Curr Opin Colloid Interface Sci* 9:201–212. <https://doi.org/10.1016/j.cocis.2004.06.008>
 15. Kanoje B, Jangir A, Patel D, Ray D, Aswal V, Pal H, Parikh J, Kuperkar K (2018) Micellar transition (ellipsoidal to ULV) induced in aqueous Gemini surfactant (12–2–12) solution as a function of additive concentration and temperature using experimental and theoretical study. *Colloids Surf, A* 555:227–236. <https://doi.org/10.1016/j.colsurfa.2018.06.070>
 16. Yawen Z, Shan W, Mengdie L, Baocai X, Fu H, Li Z (2018) Effect of temperature on the organized self-assembly of SDS/ β -cyclodextrin aqueous solution by dielectric relaxation behavior. *J Dispersion Sci Technol* 39:1056–1059. <https://doi.org/10.1080/01932691.2017.1381917>
 17. Buckingham SA, Garvey CJ, Warr GG (1993) Effect of head-group size on micellization and phase behavior in quaternary ammonium surfactant systems. *J Phys Chem* 97:10236–10244. <https://doi.org/10.1021/j100141a054>
 18. Rashidi-Alavijeh M, Javadian S, Gharibi H, Moradi M, Tehrani-Bagha AR, Shahr AA (2011) Intermolecular interactions between a dye and cationic surfactants: effects of alkyl chain, head group, and counterion. *Colloids Surf, A* 380:119–127. <https://doi.org/10.1016/j.colsurfa.2011.02.011>
 19. Jurašin D, Vinceković M, Pustak A, Šmit I, Bujan M, Filipović-Vinceković N (2013) Lamellar to hexagonal columnar liquid crystalline phase transition in a catanionic surfactant mixture: dodecylammonium chloride–sodium bis (2-ethylhexyl) sulfosuccinate. *Soft Matter* 9(12):3349–3360. <https://doi.org/10.1039/C3SM27665A>
 20. Rao KS, Gehlot PS, Gupta H, Drechsler M, Kumar A (2015) Sodium bromide induced micelle to vesicle transitions of newly synthesized anionic surface-active ionic liquids based on dodecylbenzenesulfonate. *J Phys Chem B* 119:4263–4274. <https://doi.org/10.1021/jp512805e>
 21. Bergström LM, Skoglund S, Edwards K, Eriksson J, Grillo I (2013) Self-assembly in mixtures of an anionic and a cationic surfactant: a comparison between small-angle neutron scattering and cryo-transmission electron microscopy. *Langmuir* 29:11834–11848. <https://doi.org/10.1021/la401884k>
 22. Singh M, Kumar S, Aswal VK, Kang TS (2023) Mixed aggregates of surface-active ionic liquids and 14–2–14 gemini surfactants in an aqueous medium as fluid scaffolds for enzymology of cytochrome-C. *Langmuir* 39:11582–11595. <https://doi.org/10.1021/acs.langmuir.3c01050>
 23. Mukhopadhyay A, Singh D, Sharma KP (2019) Neat ionic liquid and α -chymotrypsin-polymer surfactant conjugate-based biocatalytic solvent. *Biomacromol* 21:867–877. <https://doi.org/10.1021/acs.biomac.9b01556>
 24. Dib N, Silber JJ, Correa NM, Falcone RD (2022) Amphiphilic ionic liquids capable to formulate organized systems in an aqueous solution, designed by a combination of traditional surfactants and commercial drugs. *Pharm Res* 39:2379–2390. <https://doi.org/10.1007/s11095-022-03342-7>
 25. Kaur G, Kumar H, Singla M (2022) Diverse applications of ionic liquids: A comprehensive review. *J Mol Liq* 351:118556. <https://doi.org/10.1016/j.molliq.2022.118556>
 26. Correia DM, Fernandes LC, Martins PM, García-Astrain C, Costa CM, Reguera J, Lancers-Méndez S (2020) Ionic liquid–polymer composites: a new platform for multifunctional applications. *Adv Func Mater* 30:1909736. <https://doi.org/10.1002/adfm.201909736>
 27. Lim JR, Chua LS, Mustaffa AA (2022) Ionic liquids as green solvent and their applications in bioactive compounds extraction from plants. *Process Biochem* 122:292–306. <https://doi.org/10.1016/j.procbio.2022.10.024>
 28. Tan JS, Lee SY, Chew KW, Lam MK, Lim JW, Ho SH, Show PL (2020) A review on microalgae cultivation and harvesting, and their biomass extraction processing using ionic liquids. *Bioengineered* 11:116–129. <https://doi.org/10.1080/21655979.2020.1711626>
 29. Yan X, Anguille S, Bendahan M, Moulin P (2019) Ionic liquids combined with membrane separation processes: a review. *Sep Purif Technol* 222:230–253. <https://doi.org/10.1016/j.seppur.2019.03.103>
 30. Das S, Dutta T, Borah R (2019) Comparative study of the physical and electrochemical behavior of direct N-SO₃H functionalized 1, 3-disulfo-2-alkyl-imidazolium trifluoroacetate ionic liquids in molecular solvents. *J Mol Liq* 289:111099. <https://doi.org/10.1016/j.molliq.2019.111099>
 31. Šarac B, Medoš Ž, Cognigni A, Bica K, Chen LJ, Bešter-Rogač M (2017) Thermodynamic study for micellization of imidazolium-based surface active ionic liquids in water: effect of alkyl chain length and anions. *Colloids Surf A* 532:609–617. <https://doi.org/10.1016/j.colsurfa.2017.01.062>
 32. Dai X, Qiang X, Li J, Yao T, Wang Z, Song H (2019) Design and functionalization of magnetic ionic liquids surfactants

- (MILSs) containing alkyltrimethylammonium fragment. *J Mol Liq* 277:170–174. <https://doi.org/10.1016/j.molliq.2018.12.096>
33. Amarasekara AS (2016) Acidic ionic liquids. *Chem Rev* 116:6133–6183. <https://doi.org/10.1021/acs.chemrev.5b00763>
 34. Sarma P, Dutta AK, Borah R (2017) Design and exploration of –SO₃H group functionalized Brønsted acidic ionic liquids (BAILs) as task-specific catalytic systems for organic reactions: a review of literature. *Catal Surv Asia* 21:70–93. <https://doi.org/10.1007/s10563-017-9227-0>
 35. Buettner CS, Cognigni A, Schroeder C, Bica-Schröder K (2022) Surface-active ionic liquids: a review. *J Mol Liq* 347:118160. <https://doi.org/10.1016/j.molliq.2021.118160>
 36. Agudelo AJ, Coelho YL, Ferreira GM, Ferreira GM, Hudson EA, dos Santos Pires AC, da Silva LH (2019) Solvophobic effect of 1-alkyl-3-methylimidazolium chloride on the thermodynamic of complexation between β-cyclodextrin and dodecylpyridinium cation. *Colloids Surf A* 582:123850. <https://doi.org/10.1016/j.colsurfa.2019.123850>
 37. Selwent A, Łuczak J (2016) Micellar aggregation of Triton X-100 surfactant in imidazolium ionic liquids. *J Mol Liq* 221:557–566. <https://doi.org/10.1016/j.molliq.2016.05.081>
 38. Lu X, Lu Z, Zhang R, Zhao L, Xie H (2021) Distribution of pigments in the aqueous two-phase system formed with piperazinium-based ionic liquid and anionic surfactant. *J Mol Liq* 330:115677. <https://doi.org/10.1016/j.molliq.2021.115677>
 39. Warsi F, Usman M, Ali M (2022) Modulating aggregation behaviour and surface properties of cationic & anionic surfactant with surface active ionic liquid 1-decyl-3-methylimidazolium chloride [C10mim][Cl]: Role of surfactant head group. *J Mol Liq* 365:120093. <https://doi.org/10.1016/j.molliq.2022.120093>
 40. Zhang Y, Marlow JB, Wood K, Wang J, Warr GG, Li H, Atkin R (2023) Phase behaviour and aggregate structures of the surface-active ionic liquid [BMIm][AOT] in water. *J Colloid Interface Sci* 652:749–757. <https://doi.org/10.1016/j.jcis.2023.08.049>
 41. Beyaz A, Oh WS, Reddy VP (2004) Ionic liquids as modulators of the critical micelle concentration of sodium dodecyl sulfate. *Colloids Surf, B* 35:119–124. <https://doi.org/10.1016/j.colsurfb.2004.02.014>
 42. Behera K (2007) Pandey S (2007) Concentration-dependent dual behavior of hydrophilic ionic liquid in changing properties of aqueous sodium dodecyl sulfate. *J Phys Chem B* 111:13307–13315. <https://doi.org/10.1021/jp076430u>
 43. Behera K, Pandey S (2007) Modulating properties of aqueous sodium dodecyl sulfate by adding hydrophobic ionic liquid. *J Colloid Interface Sci* 316(2):803–14. <https://doi.org/10.1016/j.jcis.2007.07.072>. Get rights and content.
 44. Smirnova NA, Vanin AA, Safonova EA, Pukinsky IB, Anufrikov YA, Makarov AL (2009) Self-assembly in aqueous solutions of imidazolium ionic liquids and their mixtures with an anionic surfactant. *J Colloid Interface Sci* 336:793–802. <https://doi.org/10.1016/j.jcis.2009.04.004>
 45. Pal A, Chaudhary S (2013) Ionic liquid induced alterations in the physicochemical properties of aqueous solutions of sodium dodecylsulfate (SDS). *Colloids Surf, A* 430:58–64. <https://doi.org/10.1016/j.colsurfa.2013.04.001>
 46. Ferreira GM, Ferreira GM, Agudelo AJ, Hespanhol da Silva MC, Rezende JD, Pires AC, da Silva LH (2015) Effect of 1-butyl-3-methylimidazolium halide on the relative stability between sodium dodecyl sulfate micelles and sodium dodecyl sulfate–poly(ethylene oxide) nanoaggregates. *J Phys Chem B* 119:15758–15768. <https://doi.org/10.1021/acs.jpcc.5b09819>
 47. Kumar H, Katal A (2021) Thermodynamic analysis of micelles formation of anionic surfactant SDS in the presence of aqueous and aqueous solution of ionic liquid 1-butyl-3-methylimidazolium chloride. *J Phys Org Chem* 34:e4199. <https://doi.org/10.1002/poc.4199>
 48. Kumar H, Kaur G (2020) Deciphering aggregation behavior and thermodynamic properties of anionic surfactant sodium hexadecyl sulfate in aqueous solutions of ionic liquids [C5mim][Br] and [C6mim][Br]. *J Mol Liq* 298:111949. <https://doi.org/10.1016/j.molliq.2019.111949>
 49. Dutta AK, Gogoi P, Borah R (2014) Synthesis of dibenzoxanthene and acridine derivatives catalyzed by 1, 3-disulfonic acid imidazolium carboxylate ionic liquids. *RSC Adv* 4:41287–41291. <https://doi.org/10.1039/C4RA07323A>
 50. Frizzo CP, Bender CR, Salbego PR, Black G, Villetti MA, Martins MA (2016) Thermodynamic properties of the aggregation behavior of a dicationic ionic liquid determined by different methods. *Colloids Surf, A* 494:1–8. <https://doi.org/10.1016/j.colsurfa.2016.01.015>
 51. Zhao Y, Yue X, Wang X, Huang D, Chen X (2012) Micelle formation by N-alkyl-N-methylpiperidinium bromide ionic liquids in aqueous solution. *Colloids Surf, A* 412:90–95. <https://doi.org/10.1016/j.colsurfa.2012.07.021>
 52. Sohrabi B, Eivazzadeh S, Sharifi A, Azadbakht R (2015) Self-assembled cationic surfactant mixtures in aqueous/ionic liquid systems. *J Mol Liq* 211:754–760. <https://doi.org/10.1016/j.molliq.2015.07.025>
 53. Warsi F, Islam MR, Alam MS, Ali M (2020) Exploring the effect of hydrophobic ionic liquid on aggregation, micropolarity and microviscosity properties of aqueous SDS solutions. *J Mol Liq* 310:113132. <https://doi.org/10.1016/j.molliq.2020.113132>
 54. Inoue T, Ebina H, Dong B, Zheng L (2007) Electrical conductivity study on micelle formation of long-chain imidazolium ionic liquids in aqueous solution. *J Colloid Interface Sci* 314:236–241. <https://doi.org/10.1016/j.jcis.2007.05.052>
 55. Pal A, Punia R (2020) Self-aggregation behaviour of cationic surfactant tetradecyltrimethylammonium bromide and bi-amphiphilic surface-active ionic liquid 3-methyl-1-pentylimidazolium dodecylsulfate in aqueous solution. *J Mol Liq* 304:112803. <https://doi.org/10.1016/j.molliq.2020.112803>
 56. Agudelo AJ, Ferreira GM, Ferreira GM, Coelho YL, Hudson EA, dos Santos Pires AC, da Silva LH (2020) Aggregation of sodium dodecylbenzene sulfonate: weak molecular interactions modulated by imidazolium cation of short alkyl chain length. *Colloids Surf, A* 589:124435. <https://doi.org/10.1016/j.colsurfa.2020.124435>
 57. Cao H, Hu Y, Xu W, Wang Y, Guo X (2020) Recent progress in the assembly behavior of imidazolium-based ionic liquid surfactants. *J Mol Liq* 319:114354. <https://doi.org/10.1016/j.molliq.2020.114354>
 58. Rosen MJ (2004) Surfactants and interfacial phenomena: In emulsification by surfactant, page 303–31, 3rd edn. Wiley, New York
 59. Hu Y, Han J, Guo R (2020) Influence of the alkyl chain length of the imidazole ionic liquid-type surfactants on their aggregation behavior with sodium dodecyl sulfate. *Langmuir* 36(35):10494–503. <https://doi.org/10.1021/acs.langmuir.0c01673>
 60. Florence AT, Attwood D (2015) Physicochemical principles of pharmacy: In Manufacture, Formulation, and Clinical Use, page 193–244, 5th edn. Pharmaceutical press.
 61. Zhou L, Jiang X, Li Y, Chen Z, Hu X (2007) Synthesis and properties of a novel class of gemini pyridinium surfactants. *Langmuir* 23:11404–11408. <https://doi.org/10.1021/la701154w>
 62. Cheng H, Zhang H, Liu X, Lin M, Qin Z, Fang Y (2015) Effect of polyoxyethylene chain length on the physicochemical properties of n, n-dimethyl-n-dodecyl polyoxyethylene amine oxide hybrid surfactants (C₁₂EO_nAO, with n=1–4). *J Surfactants Deterg* 18:487–493. <https://doi.org/10.1007/s11743-014-1650-x>
 63. Jaycock MJ, Parfitt GD (1981) Chemistry of interfaces, page 234–247, John Wiley & Sons. New York
 64. Dong B, Zhao X, Zheng L, Zhang J, Li N, Inoue T (2008) Aggregation behavior of long-chain imidazolium ionic liquids in aqueous solution: micellization and characterization of micelle microenvironment. *Colloids Surf, A* 317:666–672. <https://doi.org/10.1016/j.colsurfa.2007.12.001>

65. Wang X, Yu L, Jiao J, Zhang H, Wang R, Chen H (2012) Aggregation behavior of COOH-functionalized imidazolium-based surface-active ionic liquids in aqueous solution. *J Mol Liq* 173:103–107. <https://doi.org/10.1016/j.molliq.2012.06.023>
66. Banjare MK, Kurrey R, Yadav T, Sinha S, Satnami ML, Ghosh KK (2017) A comparative study on the effect of imidazolium-based ionic liquid on self-aggregation of cationic, anionic, and non-ionic surfactants studied by surface tension, conductivity, fluorescence and FTIR spectroscopy. *J Mol Liq* 241:622–632. <https://doi.org/10.1016/j.molliq.2017.06.009>
67. Tanford C (1980) The hydrophobic effect: formation of micelles and biological membranes, 232 pages, 2nd edn. John Wiley & Sons. New York
68. Sharma R, Mahajan S, Mahajan RK (2013) Surface adsorption and mixed micelle formation of surface-active ionic liquid in cationic surfactants: conductivity, surface tension, fluorescence and NMR studies. *Colloids Surf, A* 427:62–75. <https://doi.org/10.1016/j.colsurfa.2013.03.023>
69. Bi Y, Zhao L, Hu Q, Gao YA, Yu L (2015) Aggregation behavior of imidazolium-based surface-active ionic liquids with photoreponsive cinnamate counterions in the aqueous solution. *Langmuir* 31:12597–12608. <https://doi.org/10.1021/acs.langmuir.5b03216>
70. Das S, Ghosh S, Das B (2018) Formation of mixed micelle in an aqueous mixture of a surface-active ionic liquid and a conventional surfactant: experiment and modeling. *J Chem Eng Data* 63:3784–3800. <https://doi.org/10.1021/acs.jced.8b00372>
71. Noriyuki M, Mariko K, Yasuko N, Shozo M, Hitoshi S (1980) Mechanism for the inducement of the intestinal absorption of poorly absorbed drugs by mixed micelles I. Effects of various lipid—bile salt mixed micelles on the intestinal absorption of streptomycin in rat. *Int J Pharm* 4(4):271–279. [https://doi.org/10.1016/0378-5173\(80\)90002-2](https://doi.org/10.1016/0378-5173(80)90002-2)
72. Seki A, Chiang K-Y, Yu C-C, Yu X, Okuno M, Hunger J, Nagata Y, Bonn M (2020) The bending mode of water: a powerful probe for hydrogen bond structure of aqueous systems. *Phys Chem Lett* 19:8459–8469. <https://doi.org/10.1021/acs.jpcllett.0c01259>
73. Vogel R, Pal AK, Jambhrunkar S, Patel P, Thakur SS, Reátegui E, Parekh HS, Saá P, Stassinopoulos A, Broom MF (2017) High resolution single particle zeta potential characterization of biological nanoparticles using tunable resistive pulse sensing. *Sci Rep* 7:17479. <https://doi.org/10.1038/s41598-017-14981-x>

Publisher's Note Springer Nature remains neutral with regard to jurisdictional claims in published maps and institutional affiliations.

Springer Nature or its licensor (e.g. a society or other partner) holds exclusive rights to this article under a publishing agreement with the author(s) or other rightsholder(s); author self-archiving of the accepted manuscript version of this article is solely governed by the terms of such publishing agreement and applicable law.